Journal of Green Energy Research and Innovation

Maximum Power Point Tracking of Solar Arrays under Partial Shading Conditions Using a New Quadratic-Spline Method

Behrooz Shaban , Abdolhossein Saleh

Highlights

- **A novel quadratic spline-based MPPT (QS-MPPT) technique accurately tracks the global maximum power point under partial shading.**
- **The method uses simple interpolation to achieve rapid, oscillation-free convergence, outperforming standard algorithms like P&O and PSO.**
- **Its low complexity enables easy implementation on cost-effective microcontrollers for real-world applications.**
- **Simulations confirm superior accuracy and speed in complex multi-peak shading scenarios compared to existing methods.**

Graphical Abstract

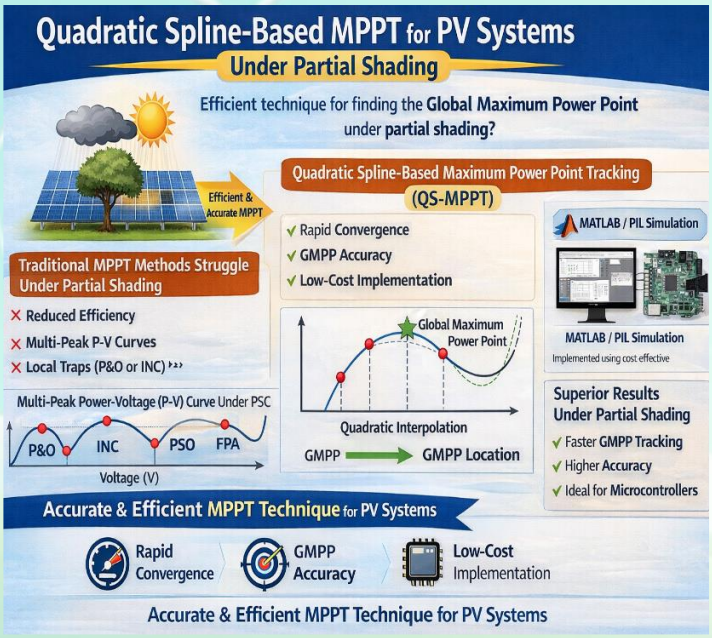

Use your device to scan and read the article online

Citation

B. Shaban, and A. Saleh, "Maximum Power Point Tracking of Solar Arrays under Partial Shading Condition Using a New Quadratic-Spline Method," *Journal of Green Energy Research and Innovation*, vol. 3, no. 1, pp. 64-76, 2026.

https://doi.org/10.61882/jgeri.3.1.64

Journal of Green Energy Research and Innovation 3.1 (2026) 64-76

Online ISSN: 3041-9018

Journal of Green Energy Research and Innovation

Journal Homepage: www.jgeri.araku.ac.ir

Maximum Power Point Tracking of Solar Arrays under Partial Shading Conditions Using a New Quadratic-Spline Method

Behrooz Shaban , Abdolhossein Saleh *

Department of Electrical Engineering, Faculty of Engineering, Malayer University, Malayer, Iran.

A R T I C L E I N F O

Keywords:
Photovoltaic Array,
Maximum Power Point Tracking,
Partial Shading Conditions,
Multi-Peak P-V Characteristics,
Quadratic Spline.

Article History:
Received: 01 September 2025;
Revised: 07 October 2025;
Accepted: 25 October 2025.

Article type:
Research Article

* ***Corresponding author***
E-mail address
hosein.saleh@malayeru.ac.ir (A.Saleh)

A B S T R A C T

Photovoltaic (PV) systems have become indispensable in the renewable energy landscape, harnessing the sun's abundant and clean potential. However, their efficiency is often compromised by low conversion rates, particularly under partial shading conditions (PSC). This study introduces a novel quadratic spline-based maximum power point tracking (QS-MPPT) technique to optimize PV array performance under both uniform irradiance and PSC. Unlike conventional methods such as Perturb and Observe (P&O) or Incremental Conductance (INC), which struggle to pinpoint the global maximum power point (GMPP) amid the multi-peak power-voltage (P-V) curves typical of PSC, QS-MPPT employs a straightforward quadratic interpolation approach. By leveraging a minimal set of sampled points, this method rapidly and accurately locates the GMPP, ensuring stability without oscillations around the operating point. Simplicity of the proposed method also makes it ideal for implementation on cost-effective microcontrollers, broadening its practical appeal for real-world PV applications. The efficiency of the proposed method is shown by the time domain simulation in the MATLAB/SIMULINK environment and implementation in the form of a processor-in-the-loop (PIL). Through MATLAB simulations, QS-MPPT performance is evaluated and compared with MPPT techniques like P&O, Particle Swarm Optimization (PSO), and Flower Pollination Algorithm (FPA) in three- and four-peak PSC scenarios, where the proposed method shows higher accuracy and faster convergence.

1. Introduction

The urgent global shift toward renewable energy has positioned photovoltaic (PV) systems as a cornerstone of sustainable power generation, capitalizing on their clean, abundant, and inexhaustible nature [1]. Solar energy offers a promising alternative to fossil fuels, reducing greenhouse gas emissions and dependency on finite resources, yet its widespread adoption is hindered by inherent limitations in energy conversion efficiency [2]. One of the most significant challenges arises under partial shading conditions (PSC), where non-uniform irradiance caused by obstacles such as buildings, trees, or clouds disrupts the uniform performance of PV arrays [3]. This disruption leads to a complex power-voltage (P-V) characteristic, marked by multiple peaks, which complicates the identification and tracking of the global maximum power point (GMPP), which is critical for optimal energy harvest [4].
Traditional maximum power point tracking (MPPT) techniques, such as Perturb and Observe (P&O) and Hill Climbing (HC), and improved methods [5,6] have been widely employed due to their simplicity and effectiveness under uniform sunlight [7]. However, these methods falter in PSC scenarios and frequently converge to local maximum power points (LMPPs) rather than the GMPP, resulting in substantial energy losses [8]. The inability of these conventional approaches to adapt to varying environmental conditions has spurred extensive research into more robust solutions [9]. Among these, advanced meta-heuristic algorithms like Particle Swarm Optimization (PSO) have gained attention for their ability to navigate multi-peak P-V characteristics by simulating swarm behavior to locate the GMPP [10]. Similarly, the Flower Pollination Algorithm (FPA) draws inspiration from natural processes to enhance tracking accuracy under challenging conditions [11], while the Artificial Bee Colony (ABC) method mimics foraging patterns to achieve comparable results [12].

- These techniques have demonstrated impressive performance, often achieving high precision and rapid convergence even in dynamic shading scenarios [13]. Despite their strengths, meta-heuristic methods come with notable drawbacks, including high computational complexity and resource demands, which inflate implementation costs and limit their practicality for widespread use, particularly in cost-sensitive applications [14]. This complexity often necessitates sophisticated hardware, posing a barrier to scalability in real-world PV installations [15]. Alternative approaches, such as Incremental Conductance (INC), aim to overcome some of these issues by relying on dynamic adjustments to track the MPP, yet they too struggle to identify the GMPP consistently under PSC [16,17]. Other strategies, like Golden Section Search (GSS), offer a structured search mechanism but lack the flexibility required for rapidly changing shading patterns [18]. Fuzzy logic-based methods have also been explored, leveraging rule-based systems to improve adaptability, though their effectiveness depends heavily on precise tuning, adding another layer of complexity [19]. In [20-22], new MPPT techniques based on the cubic spline method are presented, which are fast and accurate in tracking GMPP. These methods impose a large computational burden on the processor because they require inverting a matrix with a large number of elements to calculate the coefficients of the polynomials for each section of the P-V curve. This computational burden will be much higher when fitting multiple peaks in a multi-peak P-V characteristic in specific applications that require extracting the equivalent polynomial for all peaks. In response to these challenges, this paper introduces a novel quadratic spline-based MPPT (QS-MPPT) technique designed to balance between simplicity, accuracy, and efficiency. By employing a quadratic spline interpolation approach and establishing simplified equations, this method constructs a piecewise representation of the P-V curve using a minimal set of sampled points and provides accurate GMPP tracking without the computational overhead of meta-heuristic algorithms and the cubic-spline method. It does not involve over-fitting and the matrix inversions of higher-order splines, which are prone to ill-conditioning. The proposed technique is rigorously validated through MATLAB simulations, and its performance is compared with established methods such as FPA, PSO, and P&O, and its practical feasibility is demonstrated through processor-in-the-loop (PIL) testing using an STM32 microcontroller. Thus, the main highlights of the paper are:
- **Novel QS-MPPT algorithm:** The core contribution is a new MPPT method that uses quadratic spline interpolation to model the complex, multi-peak P-V curve that occurs under partial shading. It rapidly estimates the GMPP using a minimal set of voltage and current samples.
- **Computational efficiency and simplicity:** Unlike meta-heuristic algorithms (PSO, FPA) or cubic spline methods, the proposed quadratic approach uses simpler mathematical equations, avoiding matrix inversions and complex calculations. This makes it suitable for low-cost microcontrollers. It does not involve over-fitting and the matrix inversions of higher-order splines, which are prone to ill-conditioning.
- **Fast and accurate convergence:** Through simulations, the paper demonstrates that the QS-MPPT method converges to the GMPP faster and often more accurately than the compared methods (FPA, PSO, P&O), particularly in challenging scenarios with three and four peaks in the P-V curve.
- **Practical validation via PIL implementation:** By validating the algorithm's feasibility through PIL testing on an STM32 microcontroller, it is proven that the algorithm can be run in real-time on affordable and available hardware.

The rest of the article is divided as follows. Section 2 describes the structure of the power circuit and the PIL implementation method. Section 3 presents the concepts of quadratic spline curve fitting and the proposed MPPT method. In Section 4, time-domain simulation studies and PIL testing results are presented, and finally, in Section 5, the conclusions are drawn.

2. Power Circuit and PIL Implementation Description

The power circuit used to obtain maximum power consists of a conventional boost converter with a series array of solar panels connected to its input terminal and a resistive load at its output. The PV system design strategy varies depending on the converter and different types of loads; different criteria for resistance loads and fixed voltage loads must be considered. The structure of this circuit is shown in Figure 1.

With respect to the voltage and current gain of the boost converter, which are given in Equations (1) and (2) respectively, the relationship between the equivalent resistance observed from the load resistance R_{out} at the input of the converter R_{in} is expressed by Equation (3).

$$\frac{V_{out}}{V_{in}} = \frac{1}{1-D} \tag{1}$$

$$\frac{I_{out}}{I_{in}} = 1-D \tag{2}$$

$$R_{in} = R_{out}(1-D)^2 \; ; 0 < D < 1 \tag{3}$$

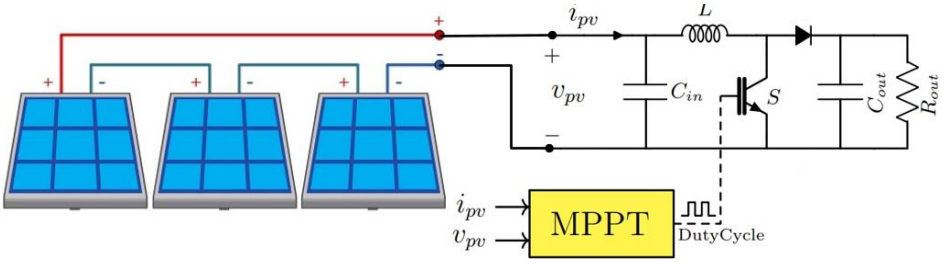

Figure 1. Power circuit for MPPT.

where V_{out}/I_{out} and V_{in}/I_{in} are respectively the output voltage/current and input voltage/current of the converter, and D is the duty cycle. Based on Equation (3), one can deduce Equation (4):

$$R_{in} \leq R_{out} \tag{4}$$

Therefore, to extract maximum power from the solar panels connected to the input of the boost converter, the load resistance must be chosen large enough so that it is greater than the equivalent resistance of the solar panel when operating at MPP. Figure 2 shows the region of the I-V characteristic of a solar panel that a boost converter can sweep at its input.

3. Concepts of Quadratic Spline Curve Fitting and Proposed MPPT Method

In this section, the concepts of curve fitting using a quadratic spline are first explained. In the following, the proposed MPPT method, derived from this curve fitting method, which can track the maximum power point in partial shading conditions in series solar panels and a multi-peaked P-V characteristic, is presented.

3.1. *Basic Concepts of Quadratic Spline Curve Fitting*

To better understand the quadratic spline curve fitting method, an explanation of the concepts of this method is provided on a hypothetical P-V characteristic shown in Figure 3. Quadratic spline interpolation defines a quadratic polynomial between two specific points; then, for the n sample points, n-1 quadratic functions are continuous and have first and second derivatives over the entire domain. For example, in Figure 3, a typical quadratic spline function connects the 5 sample points $((V_1, P_1), (V_2, P_2), (V_3, P_3), (V_4, P_4), (V_5, P_5))$ (Equations (5) and (6)), where:

$$P(v) = \begin{cases} C_1(v) & v_1 \leq v < v_2 \\ C_2(v) & v_2 \leq x < v_3 \\ C_3(v) & v_3 \leq x < v_4 \\ C_4(v) & v_4 < x < v_5 \end{cases} \tag{5}$$

where

$$C_i(v) = \gamma_i(v - v_i)^2 + \beta_i(v - v_i) + \alpha_i \;\; ; \;\; i = 1,2,3,4 \tag{6}$$

According to Figure 3, for every sample v_i, the calculated spline function should yield P_i . Then, we have Equation (7):

$$C_i(v_i) = P_i \;\; ; \;\; i = 1,2,3,4 \tag{7}$$

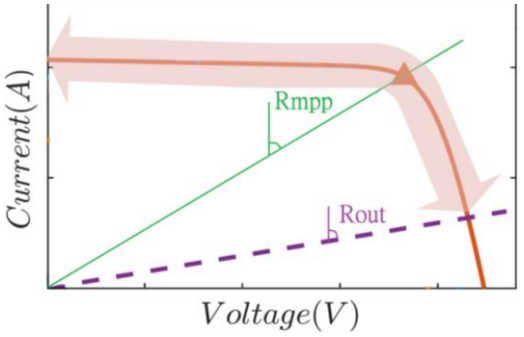

Figure 2. I-V characteristic of a solar panel and the region of the boost converter sweeping.

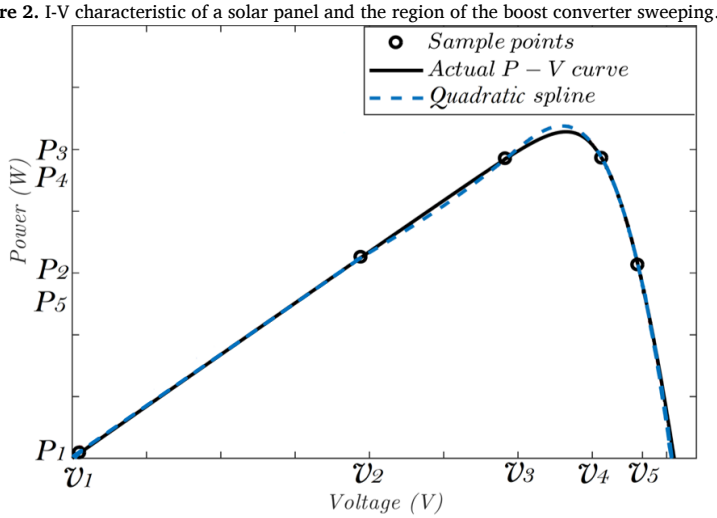

Figure 3. Hypothetical P-V characteristic and fitted quadratic spline with 5 sample points [20].

Equations (6) and (7) indicate that:

$$P(v_i) = C_i(v_i) = P_i = \alpha_i \quad ; \quad i = 1,2,3,4 \tag{8}$$

On the whole interval $[v_1, v_5]$, $P(v)$ is continuous, so as shown in Figure 3, we have Equation (9):

$$C_i(v_{i+1}) = P_{i+1} = \gamma_i(v_{i+1} - v_i)^2 + \beta_i(v_{i+1} - v_i) + \alpha_i \quad ; \quad i = 1,2,3,4 \tag{9}$$

By substituting $h_i = v_{i+1} - v_i$, Equation (10) is given:

$$\alpha_i + \beta_i h_i + \gamma_i h_i^2 = P_{i+1} \quad ; \quad i = 1,2,3,4 \tag{10}$$

Since $P(v)$ has a continuous first derivative on the interval. Therefore, the continuity of the first derivation gives:

$$C_i'(v_{i+1}) = C_{i+1}'(v_{i+1}) \rightarrow \beta_{i+1} + 2\gamma_i h_i = \beta_{i+1}$$

$$\gamma_i = \frac{\beta_{i+1} - \beta_i}{2h_i} \quad ; \quad i = 1,2,3,4 \tag{11}$$

By some manipulation in above equations, we have

$$\alpha_i + \beta_i h_i + \left(\frac{\beta_{i+1} - \beta_i}{2h_i}\right) h_i^2 = P_{i+1} \rightarrow \alpha_i + \beta_i h_i + \left(\frac{\beta_{i+1} - \beta_i}{2}\right) h_i = P_{i+1} \rightarrow 2\beta_i h_i + \beta_{i+1} h_i - \beta_i h_i = 2(P_{i+1} - P_i)$$

Thus, Equation (12) gives

$$\beta_i h_i + \beta_{i+1} h_i = 2(P_{i+1} - P_i) \; ; \; i = 1,2,3,4 \tag{12}$$

For simplicity, the curve $C_1(v)$ is fitted to a line in the interval $[v_1, v_2]$. This approximation is a proper approximation given that $C_1(v)$ lies in the linear region to the left of the peak of the P-V curve. So, we have Equation (13):

$$\gamma_1 = 0 \tag{13}$$

By substituting Equation (13) into Equation (11), we have Equation (14):

$$\beta_1 = \beta_2 \tag{14}$$

Now all other unknown coefficients in the quadratic spline functions in the interval $[v_1, v_5]$ are obtained from Equations (15)-(18):

$$\beta_1 h_1 + \beta_2 h_1 = 2(P_2 - P_1) \tag{15}$$

$$\beta_2 h_2 + \beta_3 h_2 = 2(P_3 - P_2) \tag{16}$$

$$\beta_3 h_3 + \beta_4 h_3 = 2(P_4 - P_3) \tag{17}$$

$$\beta_4 h_4 + \beta_5 h_4 = 2(P_5 - P_4) \tag{18}$$

From Equations (12) and (13):

$$\beta_1 h_1 + \beta_1 h_1 = 2(P_2 - P_1) \rightarrow \beta_1 = \beta_2 = \frac{P_2 - P_1}{h_1} \tag{19}$$

According to Equations (16)-(18), respectively, Equations (20)-(22) are deduced:

$$\beta_3 = \frac{2(P_3 - P_2)}{h_2} - \beta_2 \tag{20}$$

$$\beta_4 = \frac{2(P_4 - P_3)}{h_2} - \beta_3 \tag{21}$$

$$\beta_5 = \frac{2(P_5 - P_4)}{h_4} - \beta_4 \tag{22}$$

According to the above equations, it can be seen that the alpha values are the same as the power, and by obtaining the beta coefficients from Equations (19)-(22), the gamma coefficients can also be calculated from Equation (11). Now, by having the coefficients of the quadratic equations, namely alpha, beta, and gamma, the equations between each interval $[v_i, v_{i+1}]$, which are all quadratic, can be easily obtained with a suitable approximation. It is clear that with 5 sample points, four quadratic equations with specific coefficients will be extracted, from which the maximum value of each equation can be found.

3.2. *MPPT Method Based on Quadratic-Spline under Partial Shading Conditions*

In this section, first, the method of tracking the maximum power point using the quadratic spline-based MPPT method in atmospheric conditions with uniform radiation is explained, and then it is extended to the maximum power tracking algorithm in partial shading conditions.

A) MPPT under Uniform Irradiation

Suppose the P-V characteristic be same as that shown in Figure 3. In this case, the DC converter transfers the power generated by a single module (or a series of modules that have the same irradiations and environmental conditions) to the load. In this algorithm, only the voltage and current of the PV module are used, and no other quantities are used, which is a simple and less expensive structure. Several duty cycles (for example, 5 duty cycles) are applied to the switch by the QS-MPPT, and module current and voltage are measured to obtain the required samples and calculate their power. After collecting the required samples, the P-V curve function is approximated using the quadratic spline interpolation method to find V_{mpp} and $P_{mpp,}$ and using Equation (23), D is calculated.

$$D = 1 - \frac{V_{mpp}}{\sqrt{R_{out} * P_{mpp}}} \tag{23}$$

To further refine the outcome, an additional step involves correcting the D using a P&O algorithm with a small voltage perturbation (Δv). This crucial correction process not only enhances the accuracy of the D but also effectively mitigates the adverse effects of system non-idealities, such as parasitic resistance and forward voltage drop across diodes [20]. The algorithm operates by first identifying the optimal D and then maintaining it as long as atmospheric conditions remain stable. Should atmospheric changes disrupt the system's operating point, the PV output power will fluctuate. Consequently, the algorithm will reactivate to pinpoint a new MPP.

B) MPPT under Partial Shading Conditions

When partial shading occurs, the solar irradiation received by individual modules differs significantly. The module exposed to the most intense sunlight generates the highest current. This strong current subsequently compels modules receiving less irradiation to operate in a reverse bias state. Operating in the reverse bias region not only leads to substantial power losses but also has a detrimental impact on the PV module. Therefore, to reduce the harmful consequences of partial shading, bypass diodes are installed (Figure 4) to limit the reverse voltage across the PV modules [23].

Figure 5 illustrates an example of the characteristic curve for this PV module string under partial shading conditions, where PV_1 and PV_3 receive the highest and lowest irradiation, respectively. The activation of bypass diodes under non-uniform illumination conditions segments the P-V curve of a string into N regions, corresponding to the number of diodes. Each of these regions is characterized by a local maximum, creating a challenging multimodal optimization landscape for MPPT controllers. With only one of these points representing the global maximum (GMPP) and the other N-1 being local maxima (LMPPs), conventional tracking methods are prone to suboptimal operation. Therefore, a more sophisticated approach, like a QS-MPPT, is required to model the complex curve and precisely locate the GMPP. As illustrated in Figure 5, the P-V characteristic of a photovoltaic string comprising three modules exhibits the anticipated segmentation under varying irradiance levels, indicative of partial shading. The corresponding performance of the QS-MPPT operating under these conditions is outlined in the pseudo code presented in Figure 6. The system's electrical load is implemented via a resistive element connected to an inverter output terminal (Figure 1). During the initialization phase, the algorithm executes a sampling routine by commanding six discrete duty cycles to the power converter. It acquires the current and voltage measurements at each operating point, derives the power values, and determines the coordinates of the maximum power point (d_{max}, P_{max}). This extremum is assigned as point 4 per the reference diagram. Furthermore, the algorithm defines two auxiliary points (2' and 4') adjacent to the MPP. These are positioned along the power curve between points 3 and 4 and points 4 and 5, respectively, to refine the search domain in the subsequent iteration. The algorithm now possesses five point coordinates (1' to 5', Figure 5) and applies the QS-MPPT method. The maximum point of the approximated function is extracted, and an approximate duty cycle (D) is computed using Equation (23). A P&O algorithm (Figure 6) with a reduced step size then converges onto the exact MPP. Index $|P_{mpp}–P_{pv}|$ is defined for the final step; the algorithm continues operating at the identified D_{MPP} while this index remains below its threshold. If the index exceeds its threshold, the process re-initiates to locate a new GMPP. Continuous monitoring of photovoltaic current and voltage detects both sudden and gradual atmospheric transients that impact system performance.

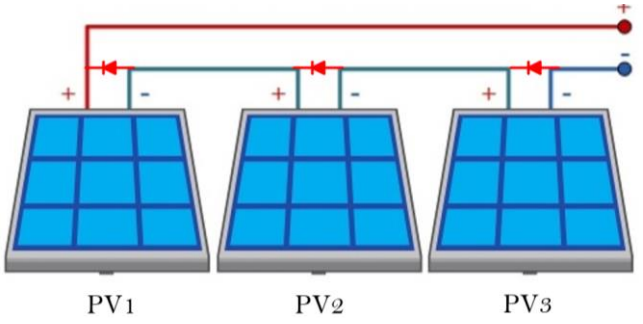

Figure 4. Three modules PV string with bypass diodes.

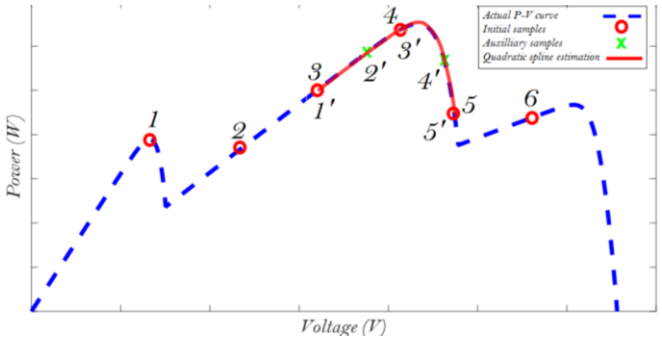

Figure 5. Curve fitting method and MPP estimation based on QS-MPPT method [20].

QS-MPPT Pseudo Code

Start

Step 1: Initial Sampling

1: create an empty set Sprimary
2: select array Dprimary with six elements
3: for (each Di in Dprimary) do
4: Apply Di to the converter and wait for steady-state.
5: Measure corresponding PV voltage Vi and current Ii.
6: Calculate power Pi = Vi × Ii.
7: Sprimary ← Sprimary ∪ (Di, Vi, Ii, Pi)
8: end for

Step 2: Identify Initial Maximum Power Point (MPP)

9: Find the sample with maximum power: (Dmax, Vmax, Imax, Pmax) ← Sprimary(max(P))

Step 3: Auxiliary Sampling

10: Identify the two neighboring duty cycles of Dmax in Sprimary.
11: create an empty set Sauxiliary
12: for (each neighbor Dneighbor) do
13: Apply a secondary duty cycle D′ (slightly offset from Dneighbor).
14: Measure (V ′, I′) and compute P′.
15: Sauxiliary ← Sauxiliary ∪ (D′, V ′, I′, P′)
16: end for
17: Stotal ← Sprimary ∪ Sauxiliary
18: Sort Stotal by voltage: Ssorted ← sortV (Stotal)

Step 4: Spline Interpolation MPP Estimation

19: Extract voltage and power arrays: V ← V (Ssorted), P ← P(Ssorted)
20: Construct a quadratic spline function fspline(V) interpolating the points (Vj,Pj).
21: Find the voltage at which fspline(V) is maximized: V mpp ← V (max(fspline(V)))
22: Estimate the corresponding power: Pmpp ← fspline(V)
23: Interpolate to find the duty cycle for Vmpp: Dmpp ← interpolate(Vmpp, Ssorted)

Step 5: Local Refinement: Apply a fine-step P&O algorithm

24: Drefined ← P&O(Dmpp, δ)

Step 6: Stability Check & Decision Logic

25: Apply Drefined to the converter.
26: Measure new operating point: (Vpv, Ipv), Ppv = Vpv × Ipv
27: if (|Pmpp − Ppv | < K) then
28: Apply Dmpp to the converter.
29: else if
30: Break to top of code in line 1, restarting global search
31: end if

End

Figure 6. QS-MPPT Pseudo Code.

3.3. Analytical Selection of Sampling Points

The selection of sampling points is designed to be systematic, rather than based on a pre-known curve. The six initial duty cycles are distributed across a wide, pre-defined range (e.g., from a minimum D_{min} to a maximum D_{max}). This ensures a coarse but comprehensive scan of the entire P-V curve. The goal is not to achieve a specific mathematical condition for the spline at this stage, but to guarantee that at least one sample lies on the curve segment containing the Global Maximum Power Point (GMPP). The auxiliary duty cycles are selected "slightly offset" from the neighbors of the D_{max} point. This densifies the sampling in the most promising region. The Quadratic Spline formulation itself inherently guarantees continuity (continuous first derivative) at the sample points through the enforcement of Equation (9) $\gamma_i = (\beta_{i+1} - \beta_i)/(2h_i)$.

This condition is built into the algorithm's core derivation and is automatically satisfied for any set of sampled points, meaning continuity and differentiability are structural features, not dependent on specific sample positions. Also, over-fitting is typically a concern with high-order polynomials. Use of low-order (quadratic) piecewise polynomials is intrinsically resistant to over-fitting. Each segment only has three coefficients and is defined by local data, preventing it from developing spurious oscillations across the entire curve. The system of equations for solving the coefficients (β_i) is a forward substitution process, Equations (19-22). It does not involve the matrix inversions of higher-order splines, which are prone to ill-conditioning.

3.4. Sensitivity Analysis ($\partial V_{mpp}/\partial Sample_i$)

In order to investigate the sensitivity $\partial V_{mpp}/\partial Sample_i$, the empirical sensitivity of the algorithm is analyzed. The extremum of a quadratic function $C_i(v) = \gamma_i(v - v_i)^2 + \beta_i(v - v_i) + \alpha_i$ is at $v_{extremum} = -\beta_i/(2\gamma_i)$.

The coefficients β_i and γ_i are linear functions of the sampled powers P_i and voltages v_i (from Equations 11, 12, 19-22). Therefore, a perturbation in a sample point will propagate linearly through the coefficient calculations, resulting in a smooth, bounded shift in $v_{extremum}$. The algorithm's robustness to this sensitivity is demonstrated in two ways:

1) Minor errors in the estimated extremum of one quadratic piece are mitigated because the algorithm selects the maximum among all quadratic pieces. An error in a non-global peak is irrelevant.

2) The final fine-step P&O stage acts as a robust corrector, locating the true physical maximum even if the spline-estimated V_{mpp} is slightly off due to sample perturbations or noise.

3.5. *Guarantee of Convergence to the Global Maximum and Robustness to Real-World Imperfections*

The proposed QS-MPPT method does not provide a strict mathematical guarantee of global convergence. Instead, its reliability is derived from a strategic sampling and robust curve-fitting strategy. The algorithm begins by sampling the entire operating range (the PV curve) with a set of six initial duty cycles. This wide-net approach is designed to ensure that at least one sample point lies on or near the curve segment containing the GMPP. The identification of the sample with the highest measured power (P_{max}) anchors the subsequent search in the most promising region. Also, the algorithm then performs auxiliary sampling around the neighbors of P_{max}. This step densifies the data points in the critical region, allowing the quadratic spline to better capture the shape of the most significant peak, including the GMPP. The impact of measurement noise, ADC quantization, and switching ripple is a crucial practical consideration. While the QS-MPPT is not immune to noise, its hybrid structure, combining a robust global estimator (spline) with a precise local tracker (P&O), makes it highly resilient. The spline provides a fast and accurate starting point very near the GMPP, and the P&O compensates for residual errors, ensuring stable and near-optimal operation even in the presence of real-world non-idealities.

3.6. *Stability Management*

The used approach to ensuring stability is based on a time-scale separation and a non-continuous operating mode. The core of stability management lies in the distinct separation between the MPPT decision-making process and the converter's steady-state operation. The QS-MPPT algorithm is not a continuous, high-frequency loop. It is an event-driven process activated only when a significant change in operating conditions is detected (i.e., when $|P_{mpp} - P_{pv}|$ exceeds a threshold K). Between these events, the converter operates at a fixed, steady duty cycle (D_{MPP}).

When holding a constant D, the boost converter with its inner inductor current loop operates as a standard, well-defined system. The stability of this mode is governed by the classic design of the converter's passive components (L, C_{in}, C_{out}) and its feedback compensator. During this prolonged steady state, the system is decoupled from the MPPT logic and is inherently stable. The sampling and proposed quadratic spline-fitting process, while more complex than P&O, is executed only during the brief MPPT event. The STM32 microcontroller has sufficient processing power to complete this calculation within a few switching cycles. This short burst of computation is treated as a transient event, not a continuous delay in a feedback loop.

Parasitic Effects (ESR, Dead Time) are non-idealities that are effectively accounted for by the hybrid P&O refinement step. The spline provides a very accurate voltage reference (V_{mpp}), and the subsequent fine-step P&O adjusts the duty cycle to achieve this voltage on the real converter, automatically compensating for parasitic voltage drops, ESR, and other non-idealities. The P&O step size is chosen to be small enough to converge without causing instability. The stability check in Step 6 of the pseudo-code ($|P_{mpp} - P_{pv}| < K$) acts as a hysteresis band. Once a new D_{MPP} is found and applied, the algorithm will not re-trigger the global search unless the power drift is significant and persistent. This prevents the algorithm from continuously resampling due to minor noise or ripple. The threshold K is set to be substantially larger than the peak-to-peak power ripple caused by switching and noise. Therefore, normal converter operation does not falsely trigger a full MPPT cycle. A resampling event only occurs due to a genuine change in irradiance. Because the system settles into a steady state for long periods, there is no continuous "reset" of the duty cycle. The transition from a fixed D to the sampling sequence and back to a new fixed D is a controlled, discrete event, not a limit cycle.

4. Simulation and PIL Results

In this section, the proposed method is applied to a photovoltaic system (Figure 7) simulated in MATLAB/SIMULINK environment.

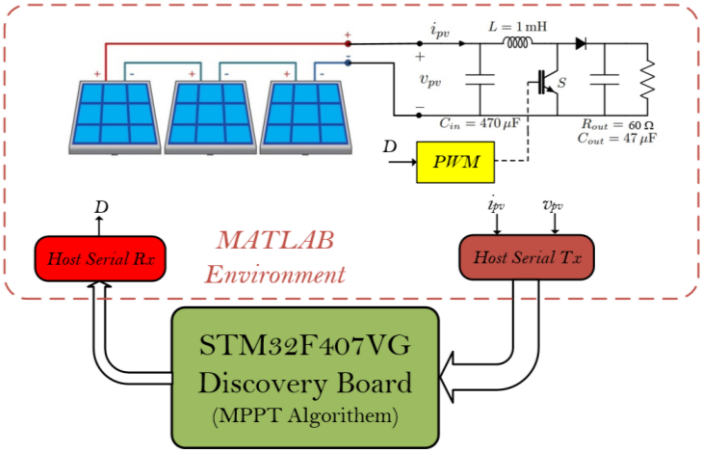

Figure 7. Power circuit and PIL implementation.

In order to investigate the feasibility of laboratory implementation of the proposed power tracking algorithm, it was built on the STM32F407VG Discovery board, which is a widely used microprocessor board [22]. Using the serial communication between this board and the MATLAB/SIMULINK environment in which the power circuit of the solar system is implemented, simulation was performed using the PIL method. As seen in Figure 7, the v_{PV} and i_{PV} quantities are sent as inputs to the processor through the serial port, and after processing these input quantities by the proposed MPPT algorithm implemented on the microprocessor, the duty cycle signal D is generated as an output and sent through the serial port to the power circuit in the MATLAB/SIMULINK environment. The parameters of the circuit are given in Table 1.

The total time required for one full MPPT cycle (T_{MPPT}) is equal to $T_{settle} + T_{sample} + T_{comput}$. Where:

1. T_{settle} (Settling Time): The time for the converter's current/voltage to stabilize after each duty cycle change. This is dictated by the converter dynamics (L, C, load).
2. T_{sample} (Sampling Time): T_{sample} = (Number of Samples) × T_{settle}.
3. T_{comput} (Computation Time): The time for the microcontroller to execute the spline fitting and maximization. This is negligible relative to T_{settle}.

The algorithm's "sampling frequency" is the inverse of the T_{MPPT} window and not periodic. To accurately track a transient, this T_{MPPT} must be shorter than the time constant of the irradiance change. In simulations and PIL tests, with a converter settling time up to ~30ms, a full MPPT cycle with 6 samples completes within 180ms. This is sufficient to track most realistic partial shading transients caused by moving clouds, which typically occur over hundreds of milliseconds to seconds. The algorithm is not designed for sub-cycle transients but for the slower, dominant shifts in the P-V curve's multi-peak structure.

In summary, the sampling strategy is robust by design, leveraging the inherent properties of quadratic splines. While formal sensitivity is a future task, the algorithm demonstrates empirical robustness. The tracking speed is practically sufficient for its intended application, as validated by simulation results.

A detailed switched model consists of three or four series solar cells. Cells are under different irradiation levels. Performance of the proposed method has been assessed in four case studies. At first, the performance of the photovoltaic system under the proposed method was evaluated when three series cell used, and these cells are under different irradiations where the irradiation also has been changed during the system operation. The second case study considered the effectiveness of the proposed method when the converter is supplied with four series solar cells with different irradiation levels. Comparison between the performance of the proposed QS-MPPT with the famous PSO, FPA-based MPPT methods, and P&O is done in the third case study done. Finally PIL implementation results are considered in forth case study.

4.1. *Case study 1: Performance of the PV system supplied with three series cells under different irradiations*

We perform the simulated scenario for two different irradiation patterns. In the first pattern, from time $t=$ 0 to $t=$ 2s, the irradiation levels for PV_1, PV_2, and PV_3 will be 1000, 800, and 600 $[\frac{W}{m^2}]$, respectively at 25 °C. In the next pattern, from time $t=$2s to $t=$4s, the irradiation intensity for PV_3 has been changed from 600 to 400 $[\frac{W}{m^2}]$ while temperature is increased to 45 °C. According to Figure 8, it can be seen that in the first stage, the power 118.87 $[W]$ is accurately tracked with $D=$ %35.06, and at time $t=$ 2s, by changing the irradiation intensity of one of the cells and increasing temperature, the proposed method accurately tracks the power and at time $t=$ 2.24s with $D=$ %57.38, it tracks the final value of 90.21 (Figure 9) $[W]$.

Table 1. Parameters of the power circuit.

Parameter	Value	Description
V_{mp}	17.145 V	For each panel
I_{mp}	3.5 A	
V_{oc}	21.1 V	
I_{sc}	3.8 A	
R_{out}	60 Ω	
L	1 mH	
C_{in}	470 μF	
C_{out}	47 μF	
Switching frequency	20kH	

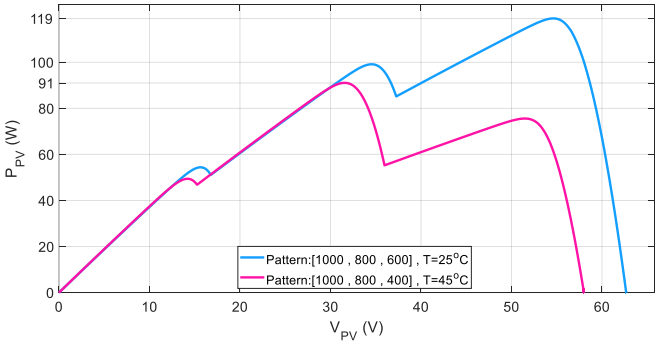

Figure 8. P-V diagram with three different radiations.

4.2. *Case study 2: Performance of the PV system supplied with four series cells under different irradiations*

In the first pattern, from time $t=0$ to $t=2s$, the irradiation levels for PV_1, PV_2, PV_3 and PV_4 will be 1000, 800, 600 and 400 $[\frac{W}{m^2}]$, respectively at 25 °C. In the next pattern, from $t=2s$ to $t=4s$, the irradiation intensity for PV_4 has been changed from 400 to 700 $[\frac{W}{m^2}]$. Figure 10 gives the P-V curves for both patterns, where for the first pattern $P_{mpp} = 117.543\ [W]$, and for the second one, the peak is shifted to $P_{mpp} = 159.22\ [W]$. According to the simulation results in Figure 10 for the first pattern of irradiation at time $t=0.24s$, the system continues to operate without oscillation with $D_{mpp}=$ %35.47. In this case, $P_{mpp}=117.13\ [W]$ at $V_{mpp}=53.62$ [V] and $I_{mpp}=2.184$ [A]. At time $t=2s$, the irradiation pattern changed to the second. In this case, the system follows the maximum power $P_{mpp}=158.81\ [W]$, with voltage $V_{mpp}=72.44\ [V]$ and current $I_{mpp} = 2.192\ [A]$, and the duty cycle also continues without oscillation with a constant value of %25.25 at t = 2.24 s (Figure 11).

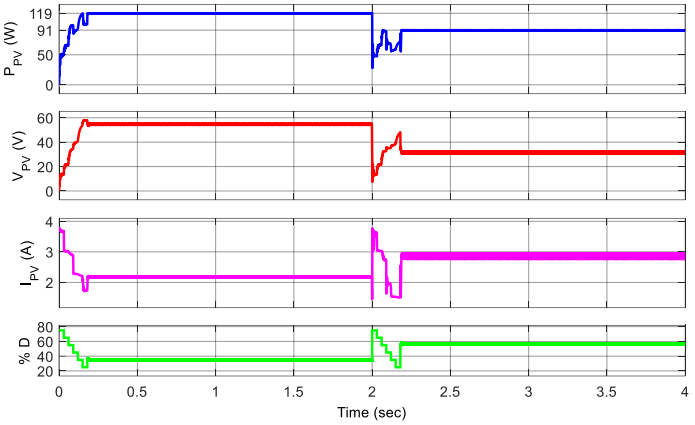

Figure 9. Simulation results under three-cell configuration.

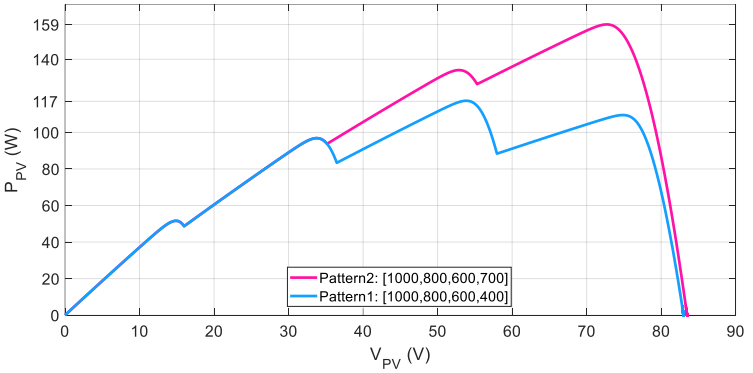

Figure 10. P-V diagram of the four-peak pattern.

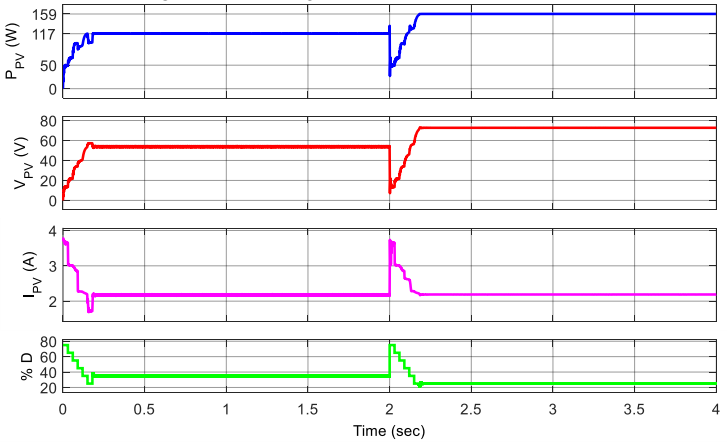

Figure 11. Simulation results under a four-cell configuration.

4.3. *Case study 3: Comparing the quadratic-spline method with P&O, FPA, and PSO-based MPPT methods*

Proposed QS-MPPT is compared with other MPPT methods, such as FPA, PSO, and P&O, in terms of accuracy and speed of convergence. All algorithms operated on the identical MATLAB/Simulink model of the PV system and power converter. The physical voltage and current bounds were the same for everyone, defined by the PV array's characteristics. In the simulation environment, all methods were subject to the same system dynamics.

Simulation results for the P-V curve shown in Figure 12 are given in Figure 13. Four series modules with irradiation intensities of 1000, 800, 600, and 400 [$\frac{W}{m^2}$] at 25 °C are connected. As is clear from the P-V curve, the power values at higher peaks are close to each other, and this proximity makes the tracking task difficult. For better comparison, simulation results for all four QS-MPPT, FPA, PSO, and P&O are presented in Table 2. It can be seen that the proposed method performs better than the other methods in terms of accuracy and speed.

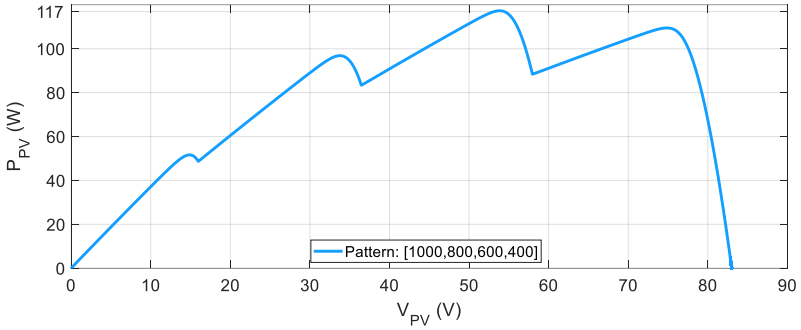

Figure 12. Four-peak diagram under partial irradiation.

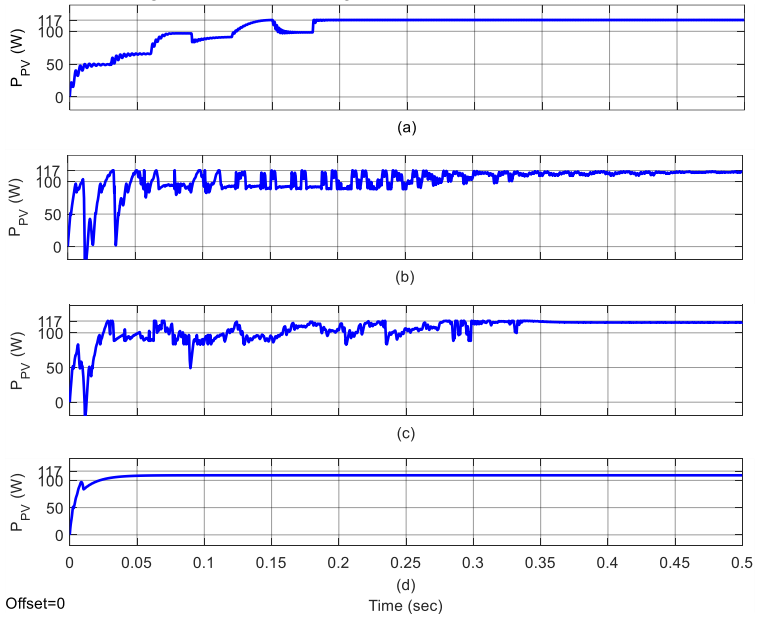

Figure 13. Power, voltage, current, and duty cycle tracking for a four-peak diagram: (a) QS-MPPT, (b) FPA, (c) PSO, and (d) P&O.

Table 2. Simulation results of QS-MPPT, FPA, PSO, and P&O methods.

	GMPP [W]	V_{mpp} [V]	I_{mpp} [A]	d_{mpp}	Tracking time [s]
Actual values	117.558	53.89	2.181	0.358	-
QS-MPPT	117.13	53.65	2.184	0.356	0.16
FPA	115.1	53.62	2.185	0.355	0.45
PSO	114.88	51.82	2.22	0.334	0.35
P&O	109.32	48.94	2.23	0.390	-

4.4. Case study 4: PIL implementation results

To assess the feasibility of implementing the proposed QS-MPPT in a laboratory setting, a PIL simulation was conducted (as shown in Figure 6). The algorithm was deployed on an STM32F407VG Discovery board microcontroller. A serial communication link was established between this hardware target and a MATLAB/Simulink software model, which contained the photovoltaic system's power circuit simulation. Within this PIL framework, the v_{PV} and i_{PV} measurements were transmitted as input parameters to the microprocessor via the serial interface. The embedded MPPT algorithm processed these inputs and computed the corresponding D. This output control signal was then returned serially to the Simulink environment to modulate the simulated power converter. The irradiation patterns at the surface of four series-connected solar cells and their parameters are respectively given in Table 3 and Table 4. Figure 14 shows the P-V curve corresponding to these patterns.

According to Figure 15, it is observed that at time 0.3 seconds, the proposed method tracks the value of 420.17 [W]. By changing the irradiation according to the pattern 2 of Table 3, the peak of the maximum power changes, but the algorithm tracks the value 566.237 [W] correctly at t= 0.6 s. Also, the irradiation intensity is changed according to the third pattern of Table 3, and it is observed that the proposed QS-MPPT method has reached the value of 270.208 [W] correctly at t= 1.2 s.

Table 3. Three different patterns for a four-peak photovoltaic system.

	Pattern 1 t=0 to 0.3 s	Pattern 2 t=0.3 to 0.9 s	Pattern 3 t=0.9 to 1.2 s
PV1	1000	1000	1000
PV2	800	800	300
PV3	600	600	600
PV4	400	700	200
P_{max} [W]	421	567	271

Table 4. Parameters of the solar cell used in the PIL implementation.

Parameter	Value	Description
V_{mp}	29 V	For each panel
I_{mp}	7.35 A	
V_{oc}	36.3 V	
I_{sc}	7.84 A	

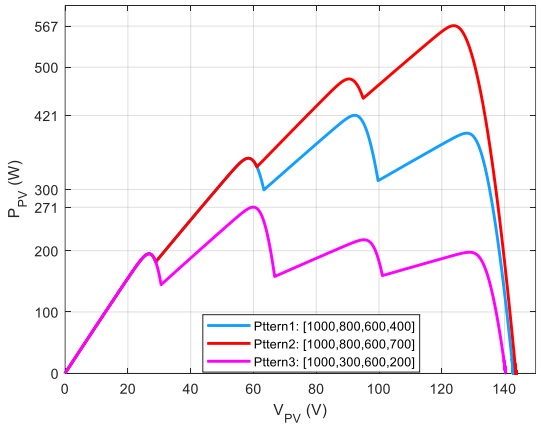

Figure 14. Four-peaked characteristics: pattern 1, pattern 2, and pattern 3.

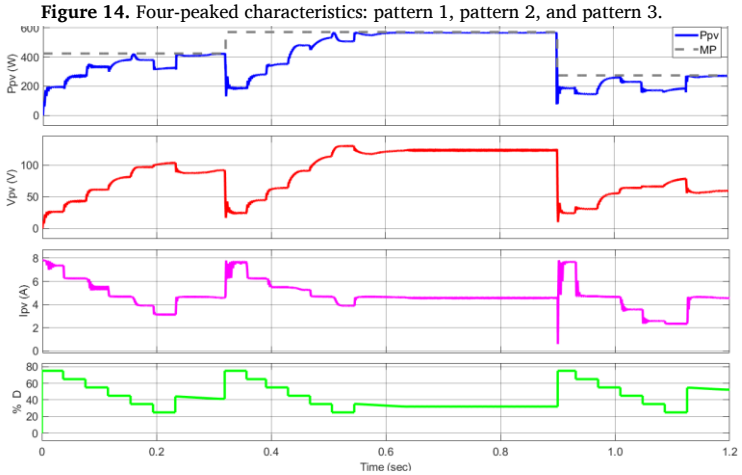

Figure 15. PIL implementation results.

5. Conclusion

In this paper, a novel QS-MPPT technique was introduced to optimize the trade-off between simplicity, accuracy, and processing efficiency. The method utilizes quadratic spline interpolation to generate a simplified, piecewise-representation of the P-V characteristic from a few measurement points, facilitating accurate GMPP estimation without the computational burden of meta-heuristic or cubic-spline alternatives. The technique's efficacy is validated through MATLAB simulations and comparative study against P&O, PSO, and FPA-based MPPT methods, and its hardware implementation viability is proven via PIL testing on an STM32 microcontroller. The results showed that this proposed method, while using simple mathematical relations to process information and find the maximum power point, tracks this point with better speed and accuracy than several other methods.

References

[1] N. D'Souza, L. Lopes, and XueJun Liu, "An Intelligent Maximum Power Point Tracker Using Peak Current Control," *IEEE 36th Conference on Power Electronics Specialists, 2005.*, 172, n.d.

[2] Weidong Xiao, and W. Dunford, "A Modified Adaptive Hill Climbing MPPT Method for Photovoltaic Power Systems," *2004 IEEE 35th Annual Power Electronics Specialists Conference (IEEE Cat. No.04CH37551)*, n.d.

[3] Y. Kim, H. Jo, and D. Kim, "A New Peak Power Tracker for Cost-Effective Photovoltaic Power System," *IECEC 96. Proceedings of the 31st Intersociety Energy Conversion Engineering Conference*, vol. 3, pp. 1673–1678, n.d.

[4] F. Ansari, S. Chatterji, A. Iqbal, and A. Afzal, "Control of MPPT for Photovoltaic Systems Using Advanced Algorithm EPP," *2009 International Conference on Power Systems*, pp. 1–6, 2009.

[5] A. Shemshadi, and H. Haghighi, "Optimal Novel Fuzzy Control Design Method for Efficient Grid-Connected Photovoltaic System," *Journal of Green Energy Research and Innovation*, vol. 2, no. 3, 2025.

[6] M. Mohseni, A. Niknam Kumleh, M. Alibakhshi, and M. Sheikhi Abou Masoudi, "Improving the Maximum Power Point Tracking in a Photovoltaic System Based on the Resistance-Predictive Method," *Journal of Green Energy Research and Innovation*, vol. 1, no. 2, pp. 81–102, 2024.

[7] P. K. Pathak, S. Padmanaban, A. K. Yadav, P. A. Alvi, and B. Khan, "Modified Incremental Conductance MPPT Algorithm for SPV-based Grid-tied and Stand-alone Systems," *IET Generation, Transmission & Distribution*, vol. 16, no. 4, pp. 776–791, 2021.

[8] R. Celikel, M. Yilmaz, and A. Gundogdu, "A Voltage Scanning-Based MPPT Method for PV Power Systems Under Complex Partial Shading Conditions," *Renewable Energy*, vol. 184, pp. 361–373, 2022.

[9] J. P. Ram, D. S. Pillai, A. M. Ghias, and N. Rajasekar, "Performance Enhancement of Solar PV Systems Applying P&O Assisted Flower Pollination Algorithm (FPA)," *Solar Energy*, vol. 199, pp. 214–229, 2020.

[10] S. R. Kiran, C. H. H. Basha, et al., "Reduced Simulative Performance Analysis of Variable Step Size ANN Based MPPT Techniques for Partially Shaded Solar PV Systems," *IEEE Access*, vol. 10, pp. 48875–48889, 2022.

[11] A. R. Nansur, F. D. Murdianto, and A. S. Laili Hermawan, "Improving the Performance of MPPT Coupled Inductor SEPIC Converter Using Flower Pollination Algorithm (FPA) Under Partial Shading Condition," *2018 International Electronics Symposium on Engineering Technology and Applications (IES-ETA)*, pp. 1–7, 2018.

[12] N. Li, M. Mingxuan, et al., "Maximum Power Point Tracking Control Based on Modified ABC Algorithm for Shaded PV System," *2019 AEIT International Conference of Electrical and Electronic Technologies for Automotive (AEIT AUTOMOTIVE)*, pp. 1–5, 2019.

[13] T. Hiyama, and K. Kitabayashi, "Neural Network Based Estimation of Maximum Power Generation from PV Module Using Environmental Information," *IEEE Transactions on Energy Conversion*, vol. 12, no. 3, pp. 241–247, 1997.

[14] K. Sakthivel, R. Krishnasamy, K. Balasubramanian, V. Krishnakumar, and M. Ganesan, "A Revolutionary Partial Resonant Inverter and Doubler Rectifier with MPPT Based on Sliding Mode Controller for Harvesting Solar Photovoltaic Sources," *Sustainable Computing: Informatics and Systems*, vol. 36, 100811, 2022.

[15] B. Yang, S. Wu, et al., "Salp Swarm Optimization Algorithm Based MPPT Design for PV-TEG Hybrid System Under Partial Shading Conditions," *Energy Conversion and Management*, vol. 292, 117410, 2023.

[16] P. K. Pathak, S. Padmanaban, A. K. Yadav, P. A. Alvi, and B. Khan, "Modified Incremental Conductance MPPT Algorithm for SPV-based Grid-tied and Stand-alone Systems," *IET Generation, Transmission & Distribution*, vol. 16, no. 4, pp. 776–791, 2021.

[17] N. R, and G. Sheela K, "Metaheuristic Algorithm Based Maximum Power Point Tracking Technique Combined with One Cycle Control for Solar Photovoltaic Water Pumping Systems," *Frontiers in Energy Research*, vol. 10, 2022.

[18] Anonymous, "A Golden Section Search Assisted Incremental Conductance MPPT Control for PV Fed Water Pump," *International Journal of Renewable Energy Research*, no. Vol12i3, 2022.

[19] T. Noguchi, and H. Matsumoto, "Maximum-Power-Point Tracking Method of Photovoltaic Power System Using Single Transducer," *IECON'03. 29th Annual Conference of the IEEE Industrial Electronics Society (IEEE Cat. No.03CH37468)*, vol. 3, pp. 2350–2355, 2003.

[20] A. Ostadrahimi, and Y. Mahmoud, "Novel Spline-MPPT Technique for Photovoltaic Systems Under Uniform Irradiance and Partial Shading Conditions," *IEEE Transactions on Sustainable Energy*, vol. 12, no. 1, pp. 524–532, 2021.

[21] C. Huang, L. Wang, et al., "A Novel Spline Model Guided Maximum Power Point Tracking Method for Photovoltaic Systems," *IEEE Transactions on Sustainable Energy*, vol. 11, no. 3, pp. 1309–1322, 2020.

[22] L. Yu, H. Wu, F. Yang, J. Jiang, and B. Deng, "Maximum Power Point Tracking (MPPT) Techniques Using Cubic Spline Interpolation – Perturb and Observe (P&O) for Partial Shading Conditions," *2024 International Symposium on Electrical, Electronics and Information Engineering (ISEEIE)*, pp. 500–506, 2024.

[23] M. Seyedmahmoudian, B. Horan, et al., "State of the Art Artificial Intelligence-Based MPPT Techniques for Mitigating Partial Shading Effects on PV Systems – A Review," *Renewable and Sustainable Energy Reviews*, vol. 64, pp. 435–455, 2016.

Declaration of competing interest

The authors declare that they have no known competing financial interests or personal relationships that could have appeared to influence the work reported in this paper. The ethical issues, including plagiarism, informed consent, misconduct, data fabrication and/or falsification, double publication and/or submission, redundancy, have been completely observed by the authors.

Bibliography

Behrooz Shaban was born in Brujerd, Lorestan, Iran. He received the Msc. degree in electrical engineering from Malayer University, Hamedan. He is currently Phd candidate at Tafresh University, Tafresh, Markazi. His research interests include switching power converters, distributed generation, and control.
Email: be.shaban66@gmail.com
ORCID: 0009-0009-8368-1430
Contribution Statement: Conceptualization, Data curation, Formal analysis, Investigation, Methodology, Software, Validation, Roles/Writing - original draft.

Abdolhossein Saleh was born in Nahavand, Hamedan, Iran, in December, 1987. He received the Ph.D. degree in electrical engineering from Bu-Ali Sina University, Hamedan, in 2019. He is currently an Assistant Professor with Malayer University, Malayer, Hamedan. His research interests include power quality, switching power converters, distributed generation, and microgrids and their control.
Email: Hosein.saleh@malayeru.ac.ir
ORCID: 0000-0002-2425-6655
Contribution Statement: Conceptualization, Data curation, Formal analysis, Investigation, Methodology, Resources, Software, Supervision, Validation, Visualization, Roles/Writing-original draft, Writing-review & editing.